

Lyotropic Liquid Crystalline Phase Behaviour in Amphiphile-Protic Ionic Liquid Systems

Zhengfei Chen,^{1,2} Tamar L. Greaves,² Celesta Fong,² Rachel A. Caruso,^{1,2*} Calum J. Drummond^{2*}

¹ PFPC, School of Chemistry, The University of Melbourne, Melbourne, Victoria, 3010, Australia

² CSIRO Materials Science and Engineering, Bag 10, Clayton South MDC, VIC 3169, Australia

*To whom correspondence should be addressed.

R. A. Caruso, Email: rcaruso@unimelb.edu.au

C. J. Drummond, Email: calum.drummond@csiro.au

Supplementary information

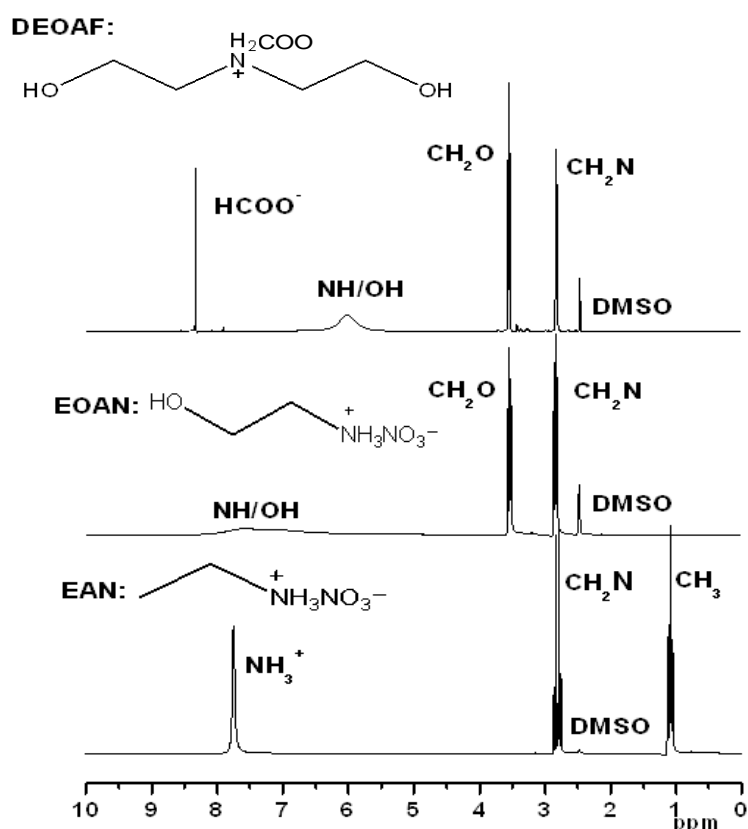
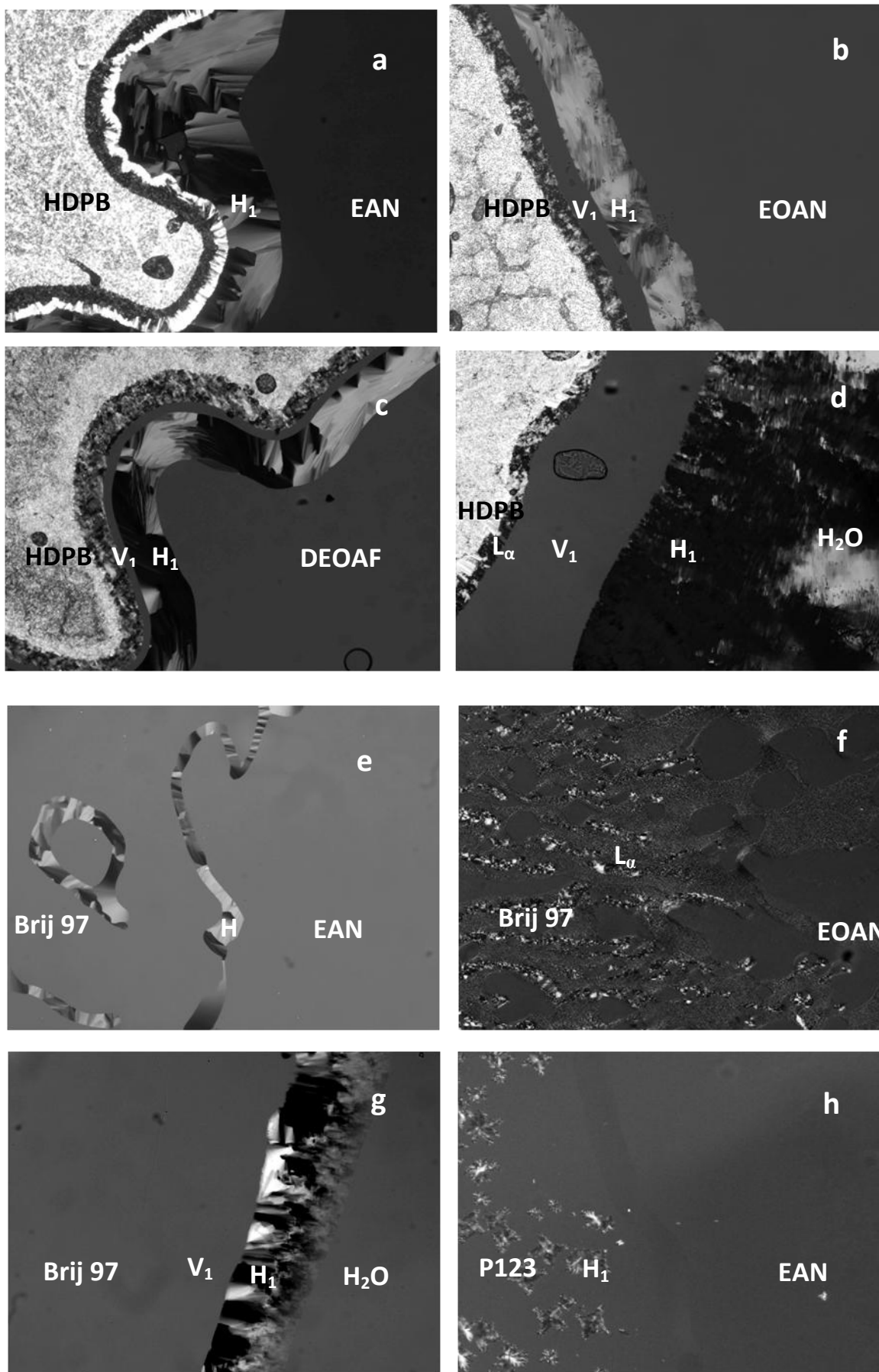


Figure S1. ¹H NMR spectra of EAN, EOAN and DEOAF. Note: the broad peaks in the EOAN and DEOAF spectra were due to the average value of NH and OH peaks, in which the protons were exchangeable and undistinguishable. The NH/OH peak in EOAN was at higher chemical shift than that in DEOAF, which was caused by the fact that EOAN was formed by a strong acid (higher pKa value).



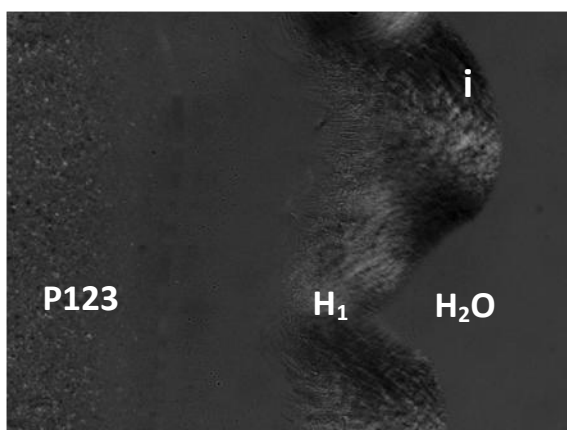


Figure S2. Cross polarised optical microscopy images of penetration scans of various amphiphile-PIL and amphiphile-water systems, neat amphiphile on the left and neat PIL or water on the right. a) HDPB-EAN; b) HDPB-EOAN; c) HDPB-DEOAF; d) HDPB-H₂O; e) Brij 97-EAN; f) Brij 97-EOAN; g) Brij 97-H₂O; h) P123-EAN; and i) P123-H₂O;. Note: images a to d were taken at 60 °C, images f to i were taken at 45 °C. (Magnification: 100X)

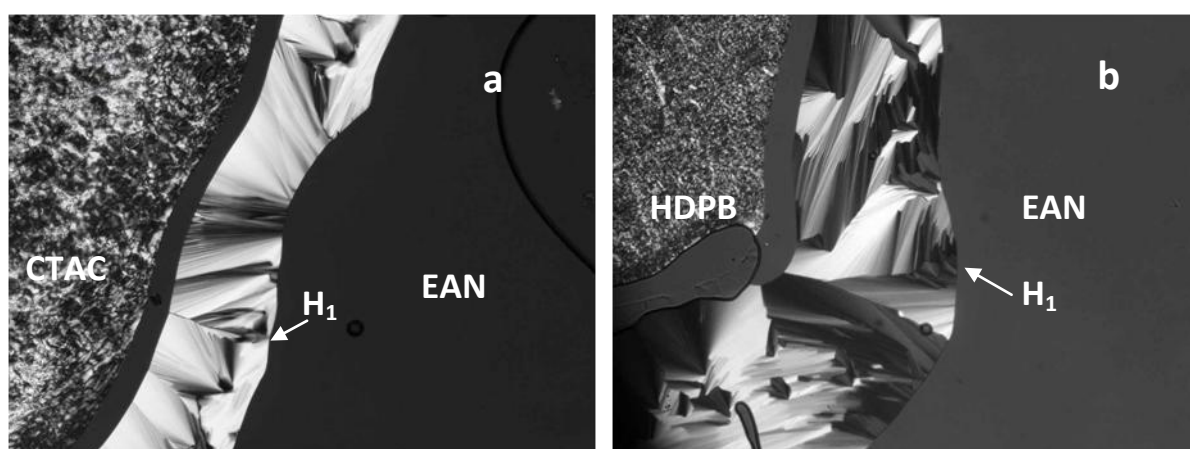


Figure S3. Cross polarised optical microscopy images of penetration scans of PIL-surfactant systems at 90 °C for a) CTAC-EAN and b) HDPB-EAN (neat surfactant on the left and neat PIL on the right). This shows the high thermal stability of the liquid crystalline phase. (Magnification: 100X)

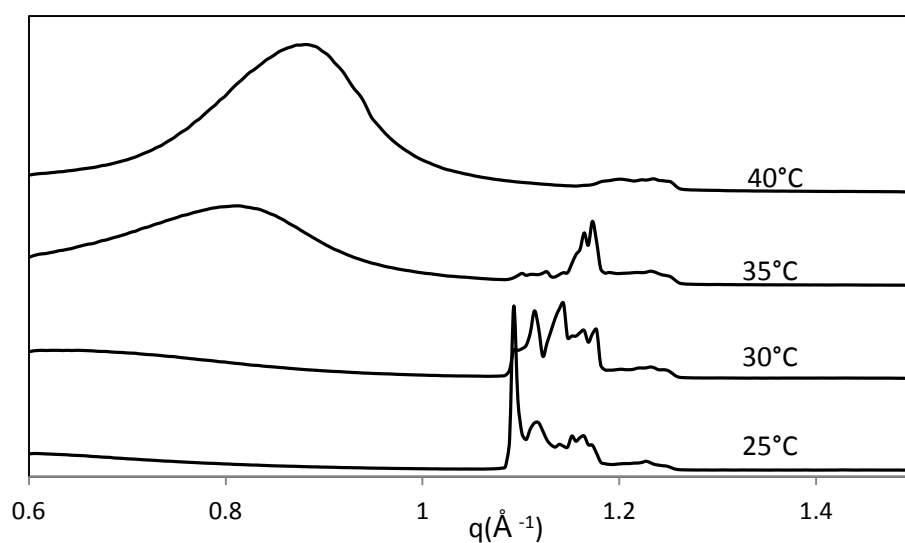
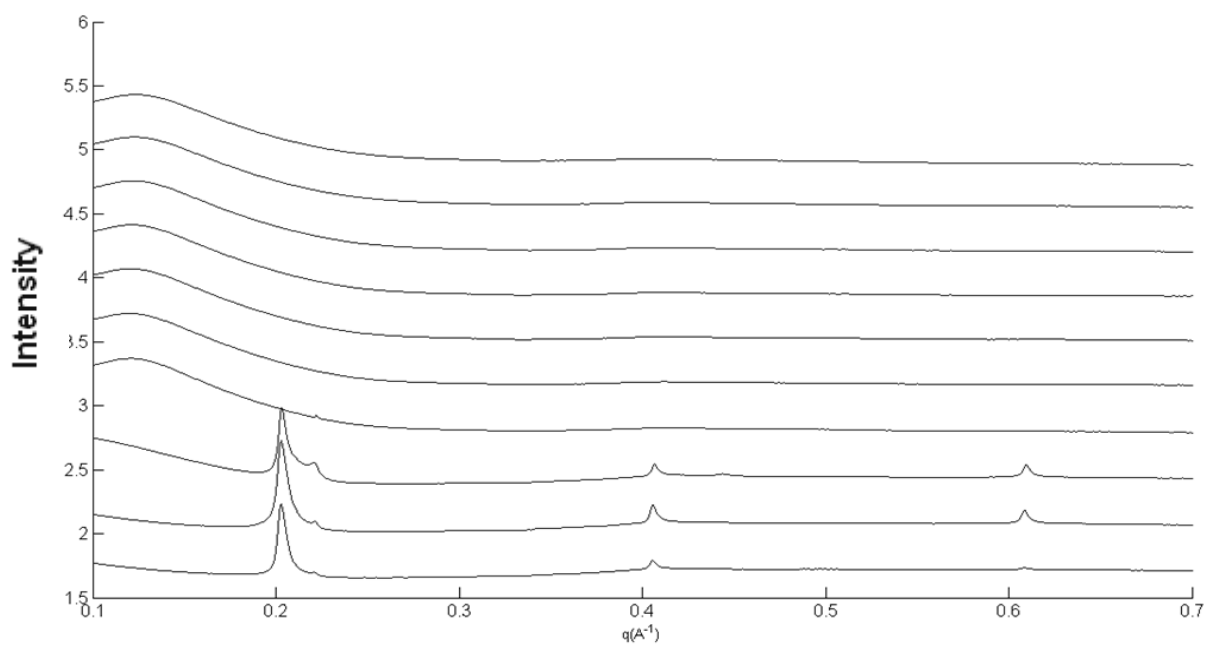
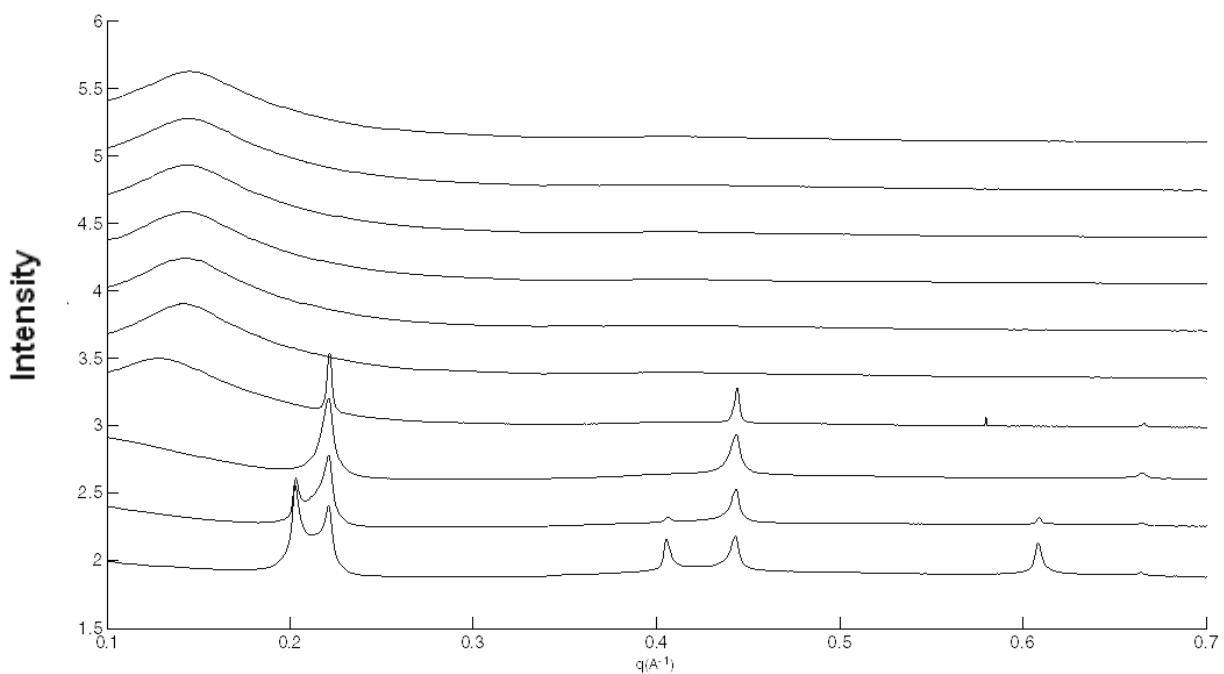


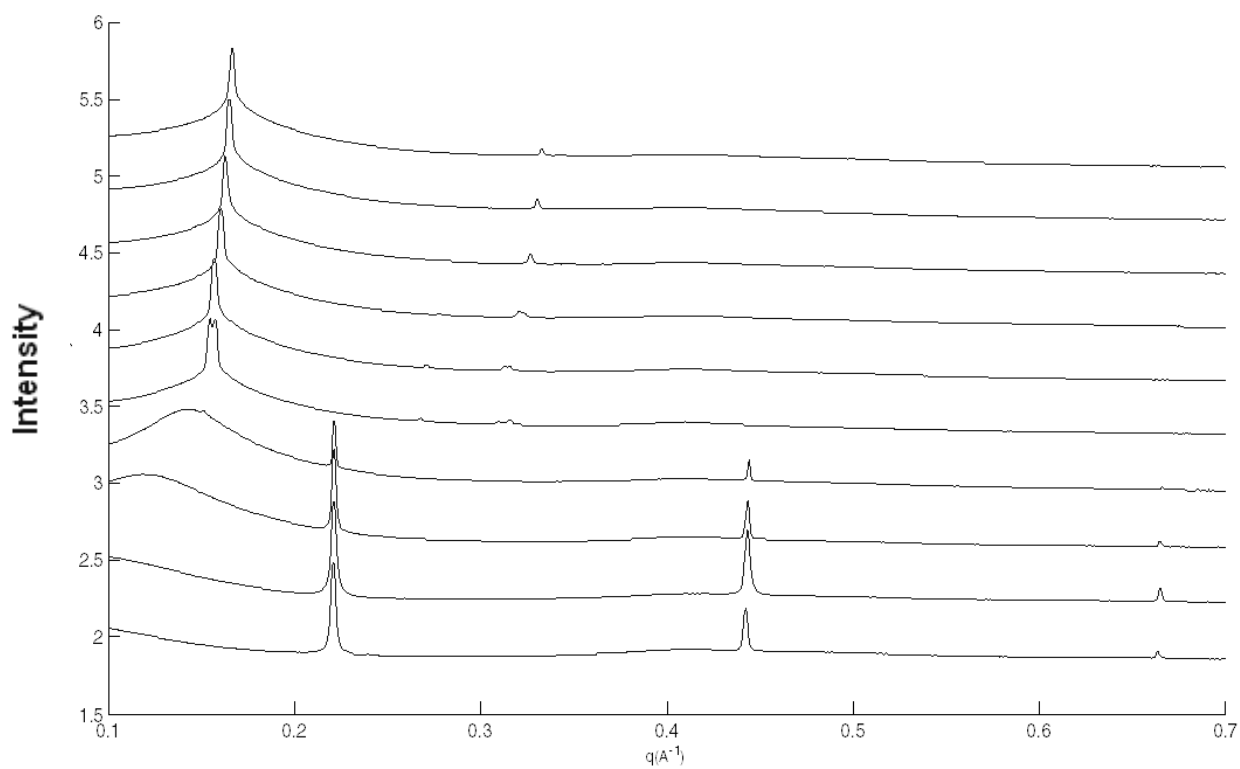
Figure S4. Representative WAXS patterns for 60 wt% CTAC in EAN at various temperatures, showing disappearance of the L_C peaks due to melting of the lamellar crystals at temperatures > 35 °C.



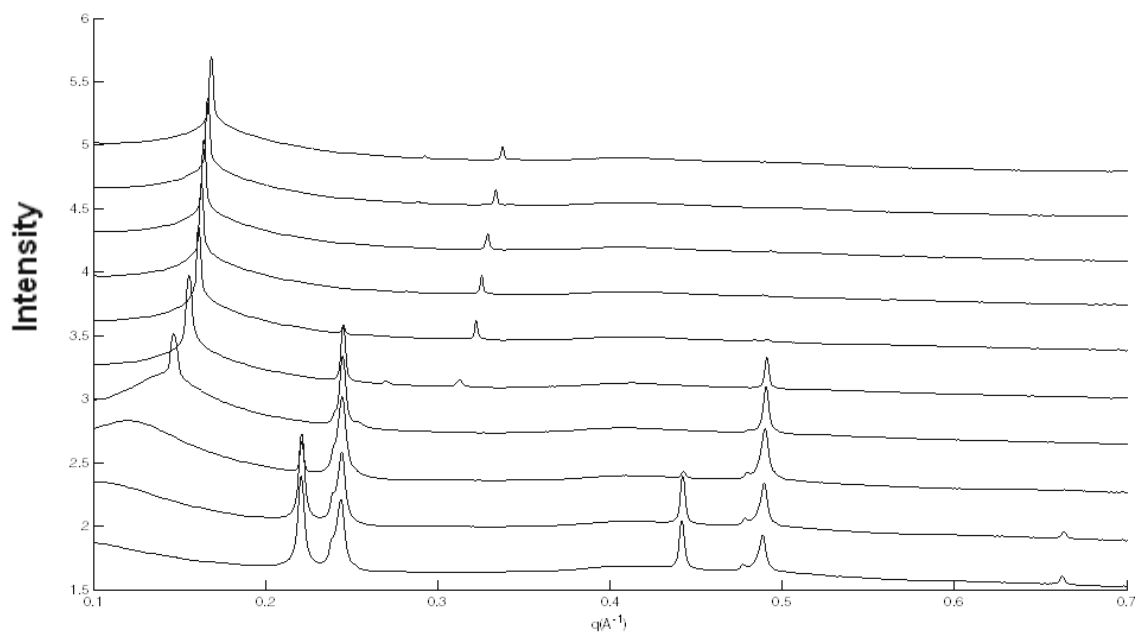
20 wt% (crystal to micellar phase)



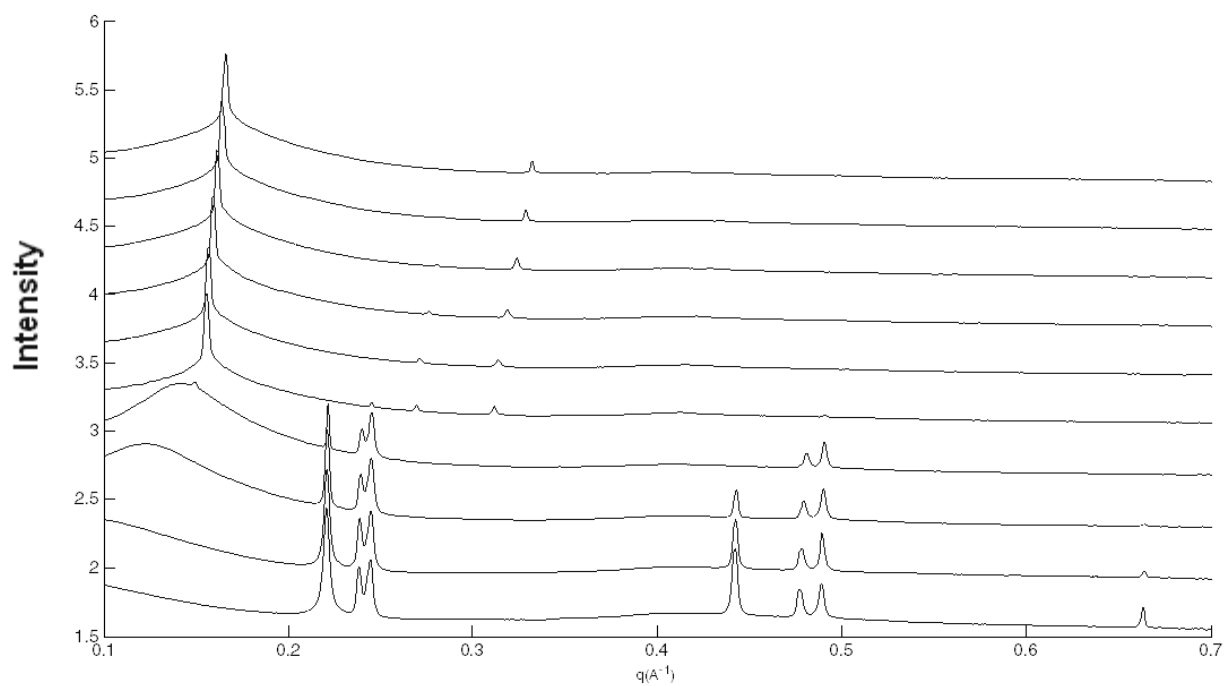
40 wt% (crystal to micellar phase)



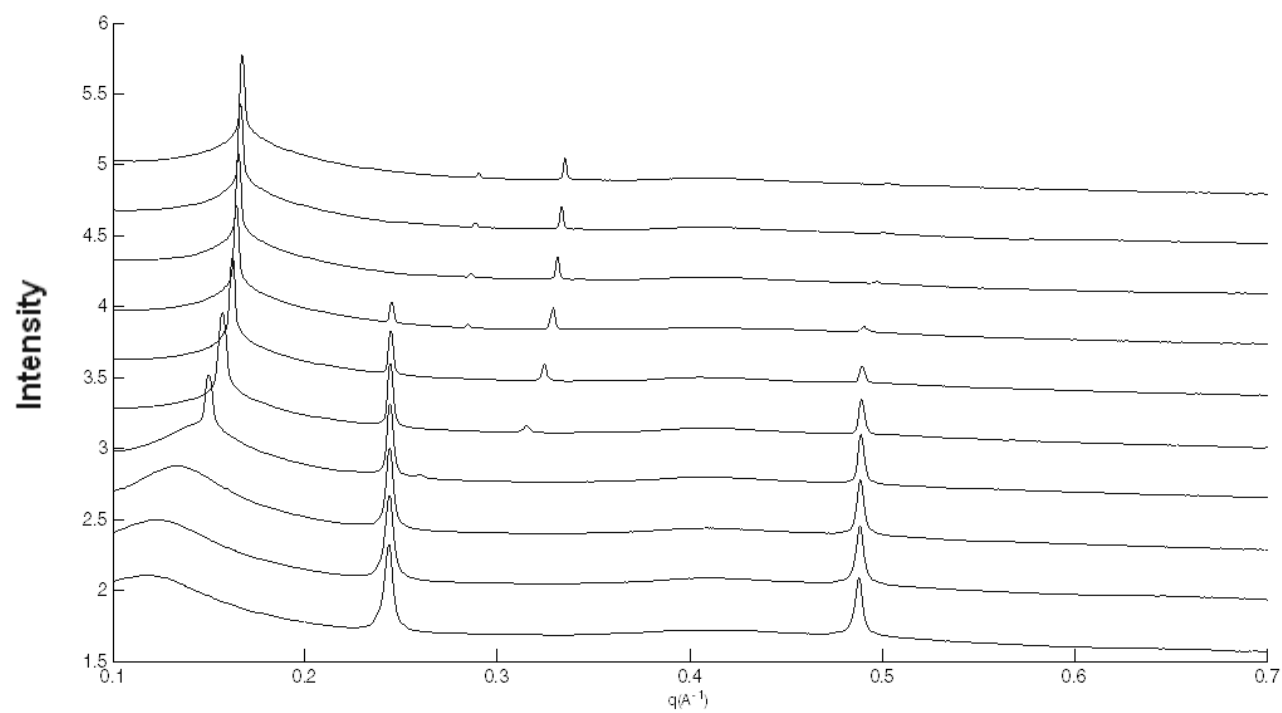
50 wt% (crystal to hexagonal phase)



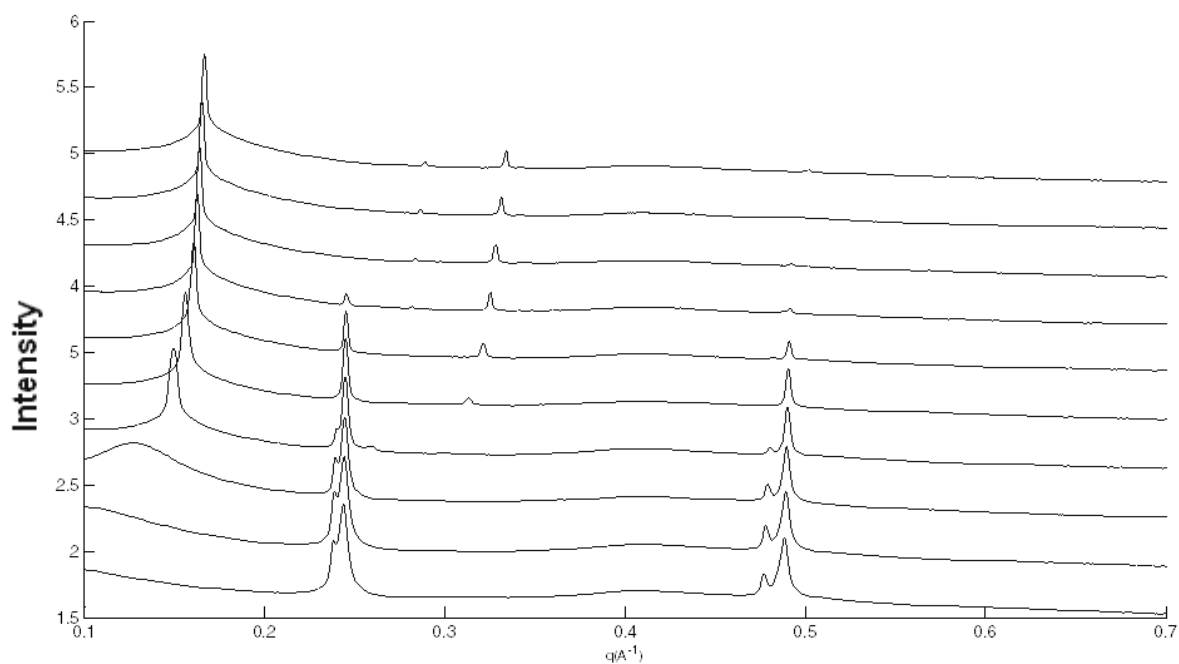
60 wt% (crystal to hexagonal phase)



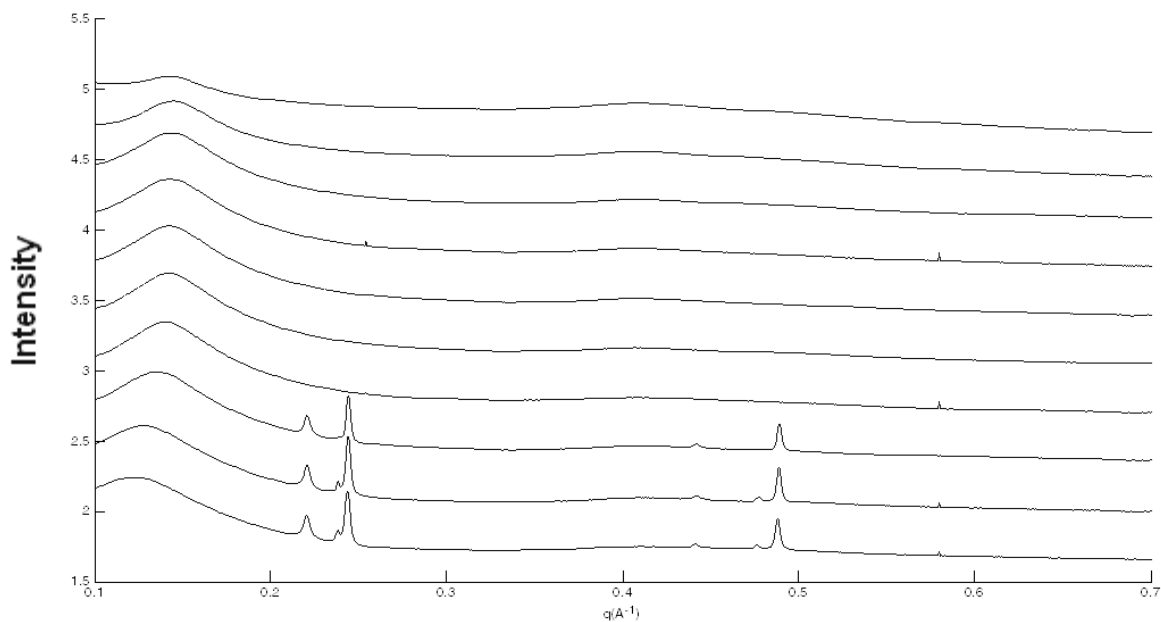
65 wt% (crystal to hexagonal phase)



70 wt% (crystal to hexagonal phase)



75 wt% (crystal to hexagonal phase)



80 wt% (crystal to isotropic phase)

Figure S5. SAXS patterns of CTAC-EAN series. Temperatures in each composition were increased from 25 °C to 70 °C in a step of 5 °C (from the bottom to the top).

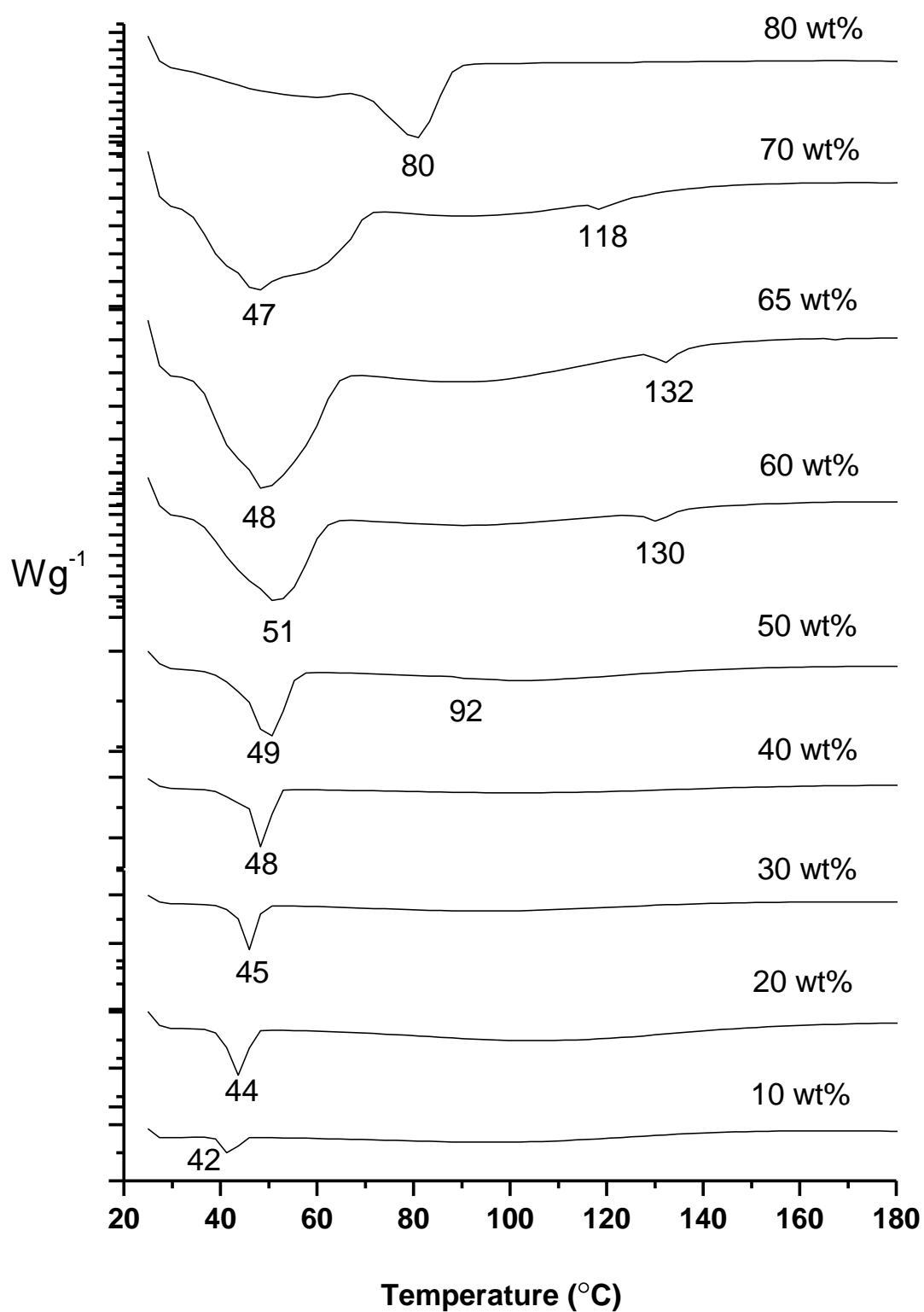


Figure S6. DSC curves of CTAC-EAN series. The first endothermic peak and the second endothermic peak refer to the melting of CTAC crystals and lyotropic crystalline liquid hexagonal phase, respectively.

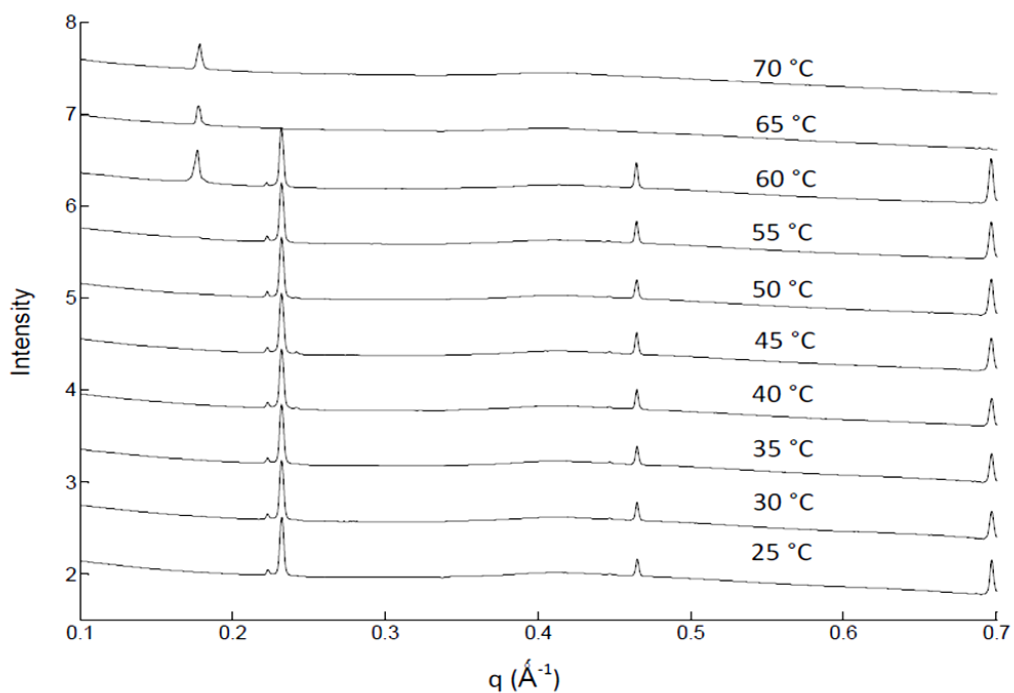


Figure S7. SAXS patterns of neat CTAC at various temperatures, showing the lamellar crystals below 60 °C and the formation of short range ordering above 60 °C.

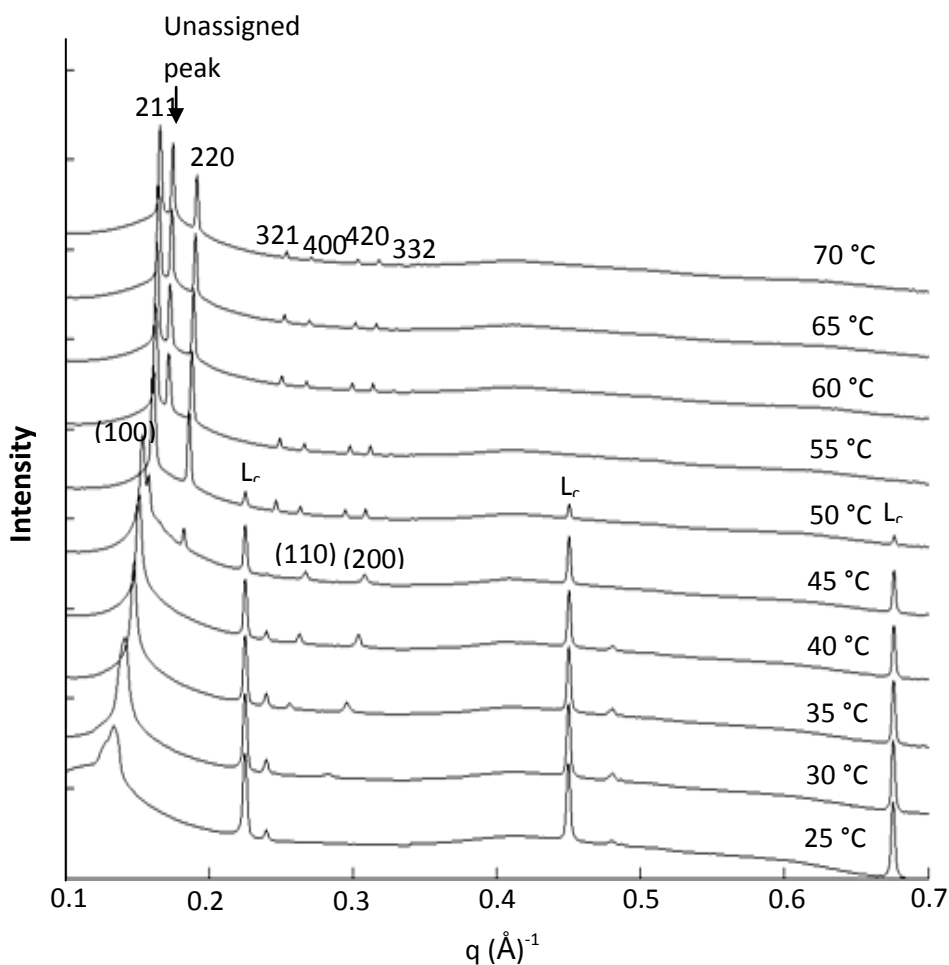


Figure S8. SAXS patterns for 80 wt% CTAC in DEOAF at various temperatures, showing the change of structures. The index numbers in brackets denote the H₁ phase while the numbers without bracket are for the cubic phase, V_I. L_c indicates a surfactant lamellar crystal phase.

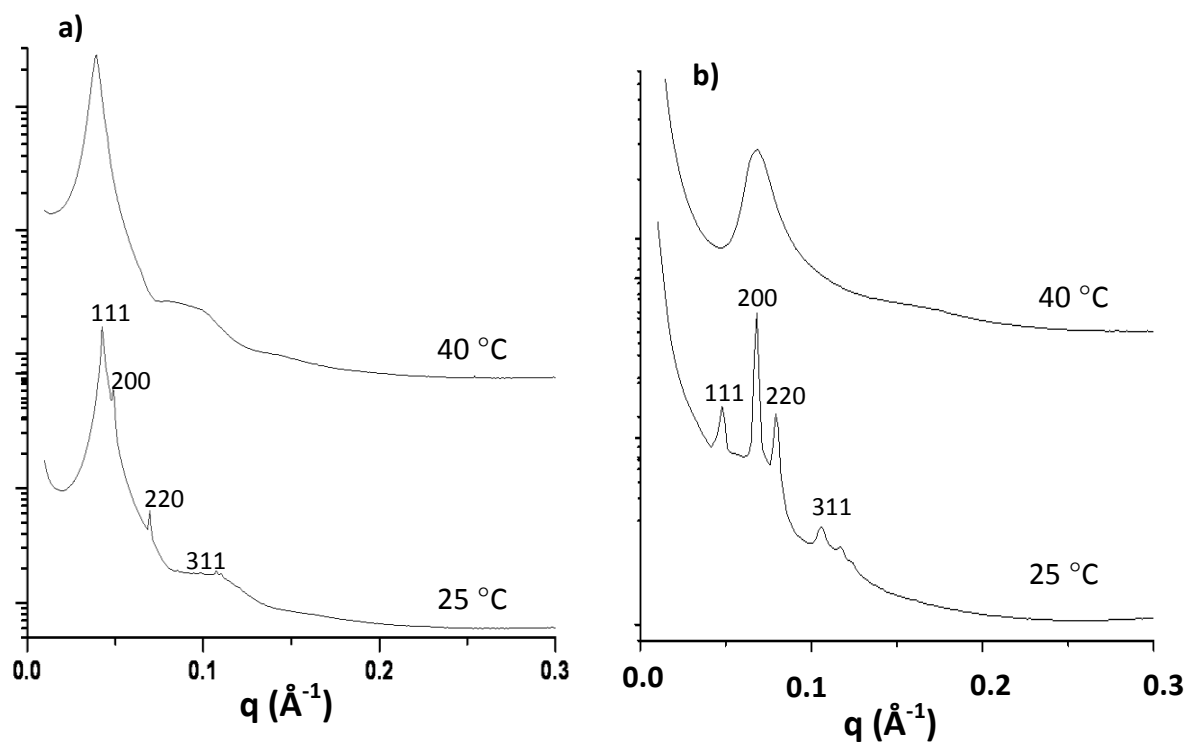


Figure S9. SAXS patterns for a) 30 wt% P123 in EAN and b) 30 wt% P123 in water at 25 and 40 °C. The peaks are indexed and assigned to a Fm3m phase.

Table S1 d-spacing value (Å) for the hexagonal phase at 45 °C.

	Concentration (wt%)	Hexagonal (H ₁)			
		EAN	EOAN	DEOAF	Water
CTAC	40	--	--	45.0 (0.140)	--
	50	41.4 (0.152)	--	42.8 (0.147)	44.7 (0.141)
	60	40.5 (0.155)	48.9 (0.128)	41.4 (0.152)	41.8 (0.150)
	70	40.3 (0.156)	47.1 (0.133)	40.9 (0.154)	41.0 (0.153)
HDPB	50	40.4 (0.156)	51.8 (0.121)	42.4 (0.148)	47.4 (0.133)
	60	38.7 (0.162)	46.7 (0.135)	42.7 (0.149)	43.7 (0.144)
	70	37.7 (0.167)	43.5 (0.144)	42.2 (0.147)	41.8 (0.150)
Brij 97	30	--	--	Immiscible	83.3 (0.075)
	40	--	--		71.2 (0.088)
	50	53.3 (0.118)	--		64.6 (0.097)
	60	51.9 (0.121)	--		--
	70	51.1 (0.123)	--		--
P123	40	136.3 (0.046)	Immiscible	Immiscible	146.3 (0.043)
	50	135.3 (0.046)			137.3 (0.046)
	60	127.4 (0.049)			128.6 (0.049)

Note: The numbers in brackets are the corresponding q values (\AA^{-1}) of their d-spacings. H₁ denotes hexagonal phase and "--" indicates the hexagonal phase was not detected. The d-spacing (d_{100}) was calculated as $d_{100} = 2\pi/q$.

Table S2 d-spacing values (Å) and their corresponding q values for the cubic (d_{211}) and lamellar (d_{100}) phases.

	Cubic (V_1)			Lamellar (L_α)		
	EOAN	DEOAF	Water	EAN	EOAN	Water
CTAC	42.3 (0.149) ^d	40.3 (0.156) _d	39.0 (0.161) ^d	--	--	--
HDPB	40.3 (0.156) ^d	39.3 (0.160) ^d	--	--	--	--
Brij 97	--	--	62.2 (0.101) ^a 60.4 (0.104) ^b	--	61.7 (0.102) ^a 56.5 (0.111) ^c 54.4 (0.115) ^d	59.0 (0.106) ^c 59.8 (0.105) ^d
P123	--	--	--	114.0 (0.055) ^c 108.2 (0.058) ^d	--	118.2 (0.053) ^c 107.2 (0.059) ^d

Note: The numbers in brackets are the corresponding q values (Å^{-1}) of their d-spacings. a, b, c, d indicate the surfactant weight concentrations at 60 wt%, 65 wt%, 70 wt% and 80 wt%, respectively. All d-spacing values for the cubic phase were calculated above 45 °C except for Brij 97 where they were calculated at room temperature. "--" indicates the lamellar phase was not detected. The d-spacing (d_{211} or d_{100}) was calculated as d_{211} (or $d_{100}) = 2\pi/q$.